Pakistan J. Sci. Ind. Res., Vol. 21, Nos. 3-4, June - August 1978

QUANTITATIVE DIMENSIONAL CHARACTERIZATION OF POLYMER SINGLE CRYSTALS FROM THEIR LIGHT SCATTERING IN STREAMING SYSTEMS

NOOR AHMAD

Institute of Physical Chemistry, University of Peshaswar, Peshawar

(Received March 8, 1977)

Abstract. Light scattering by nonspherical particles which are oriented by streaming furnishes a method for investigating the size and shape of the scattering materials [1-4]. A new experimental technique used for this investigation is the measurement of the change in the intensity of the light scatterd by polymer single crystals when they are oriented by a velocity gradient. The systems investigated consist of suspension of polymer single crystals of polyethylene. The estimated lengths are found to be within the range of the expected value as determined independently by electron microscopy.

INTRODUCTION

The light scattering method at rest are relatively insensitive to particle shape, since the effect observed at a given angle of observation, in a system at rest, is the average of all possible orientations of the nonspherical bodies. By this averaging, characteristic effects of nonspherical shape upon light scattering are lost.

The orientation of the particle can be achieved by applying an electric field, a magnetic field, or velocity gradient in laminar flow. Hydrodynamic orientation was selected in the present case. The theory of this type of orientation in three dimensional system was developed by Peterlin and Stuart [5]. Because of the importance of the velocity gradient in hydrodynamic orientation, an experimental set up is desirable in which the gradient is constant, or nearly so, perpendicular to the direction of flow. This condition is fulfilled by the gap between the two concentric cylinders, of which one is rotating and the other is stationary. The theory of this arrangement for the case of stationary outer cylinder, used in the present investigation, is due to Taylor [6].

The particles which tend to be oriented in the direction of flow lines due to the rotation of the inner cylinder of concentric cylinder apparatus, are also acted upon by the random forces of the rotatory Brownian motion, which tend to upset the flow-induced orientations. This opposing force is described by a rotational diffusion constant (D_r) which is a function of particle shape and size. At a given velocity gradient G, rotatory Brownian motion and the torque on the particle due to the velocity gradient balance out to produce an uneven rotation of the particle about its minor axis in which it spends more time at a certain preferred angle with respect to the stream lines than at any other. The higher the velocity gradient, the longer period of time the particle will dwell at that angle and closer that angle will be to stream lines. The relationship between this preferred angle, velocity, diffusion constant and axial ratio has been put on exact theoretical basis by Peterlin and Stuart [5]. Scheraga Edsall and Gadd [7] have tabulated the values of extinction angle χ (the angle which characterizes the orientation of an anisometric particle with respect to the direction of the velocity gradient, and which is to be expected in terms of the axial ratio, p, and the parameter $\beta = G/D_r$. After experimentally finding the value of D_r, the length of the crystals can be calculated by taking the electron microscopic values of axial ratio p and using Gan's [8] equation for the calculation of D_r for prolate spherids $P > 1$.

APPARATUS

The apparatus consists of the concentric cylinder assembly and the optical system.

I. *Concentric Cylinder Assembly.* The assembly (Fig. 1) supported vertically consists of two coaxial cylinders of which only the inner cylinder rotates. The annulus between the cylinders can be varied from 0.2 to 0.8 mm by suitable choice of the rotor (inner cylinder). This assembly, built almost entirely of stainless steel, has two openings (1,2 in Fig. 1) parallel to the axis of cylinder unit, providing for the incident and transmitted light beam through the annulus. A third main opening situated in the outer wall (3) allows for the measurement of the scattered light intensity of dispersed solute in the annulus.

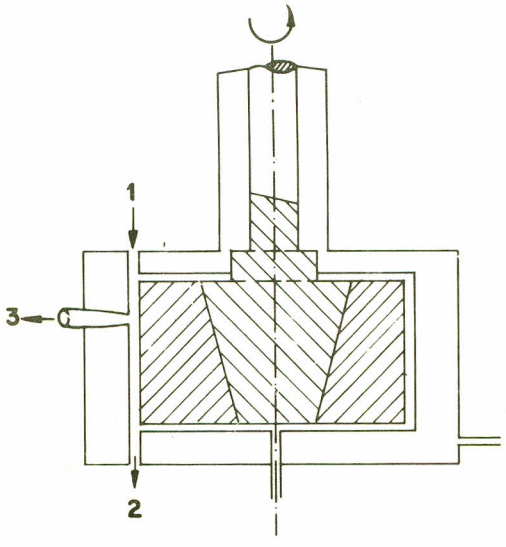

Fig. 1. The concentric cylinder assembly.

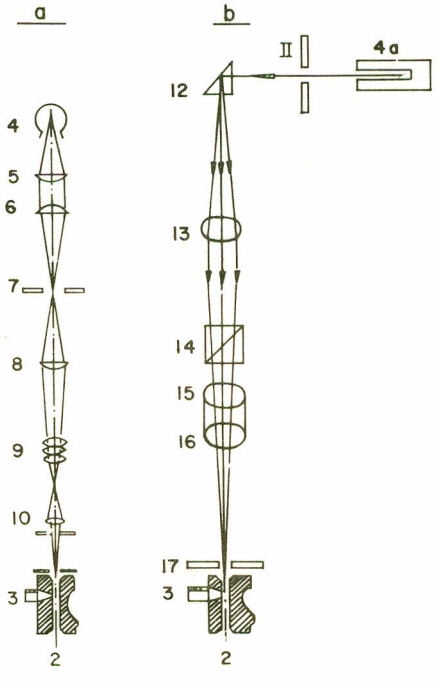

Fig. 2. Optical system: (a) Hg-arc lamp as a light source; (b) Laser as a light source.

II. *The Optical System.* The optical system can be further subdivided into two parts, depending upon the light source being used.

Fig. 2 a describes the light source (4), a water cooled AH-6 Hg Arc lamp (mounted vertically). The optical accessories are a collimating unit (lenses 5 and 6), a double slit (7) and two additional lenses (8,9). Lenses (9) are actually a low power microscope objective consisting of three small lenses. A Nicol prism (10) is also housed in the holder of lenses (9).

When laser (4a) (He-Ne gas laser of wavelength 6328 Å) is used as a light source, then the schematic drawing of the optical system is as shown in Fig. 2b.

The optical accessories consist of a slit (II), a prism (12), a convexing lens (13) or 50 cm in focal length, a polarizer (14), two quarter wave plates (15 and 16); and another slit (17) is used just before the light beam enters the annular space.

CRYSTALS INVESTIGATED AND THEIR MODE OF PREPARATION

The polymer single crystals used in this study were of polyethylene [9,10]. The material used for their preparation was linear polyethylene of low molecular weight known under the trade name of Marlex 6050.* The concentration of the polymer was varied from 0.01 to 0.5% and was dissolved in the boiling solvent xylene (at 141.5°) Crystallization at high temperature and low concentration gives simple lozenges, decrease of temperature and increase of concentrations tends to produce dendritic crystals. Low molecular weight of Marlex is quite suitable for diamond-shaped crystals.† Fig. 3 shows a representative electron micrograph of one of these crystals. The crystals are diamond shaped, very large in two dimensions. Their axial ratio 1.5 ± 0.1 is quite constant at all the temperatures and the different sizes of the crystals obtained at various temperatures and concentrationsare given in Table 1.

Table 1. Size range of the polyethylene crystals obtained at various temperatures and concentrations, as determined by electron microscopy.

Sample	Temp °C	Concn %	Size range μ
I	76	0.497	7.5 ± 4.3
II	80	0.231	5.3 ± 2.9
III	84	0.104	4.4 ± 2.5
IV	87	0.0987	4.1 ± 2.3
V	90	0.083	3.9 ± 2.05
VI	92	0.031	3,7 ± 1.8

* Marlex 6050 is a high density polyethylene made by Philips Petroleum Company, Bartlesville, Oklahoma, U.S.A.

† Dr. J.H.L. Watson of the Physics Dept. of the Edsell B. Ford Institute for Medical Research, Detroit, U.S.A., personal communication

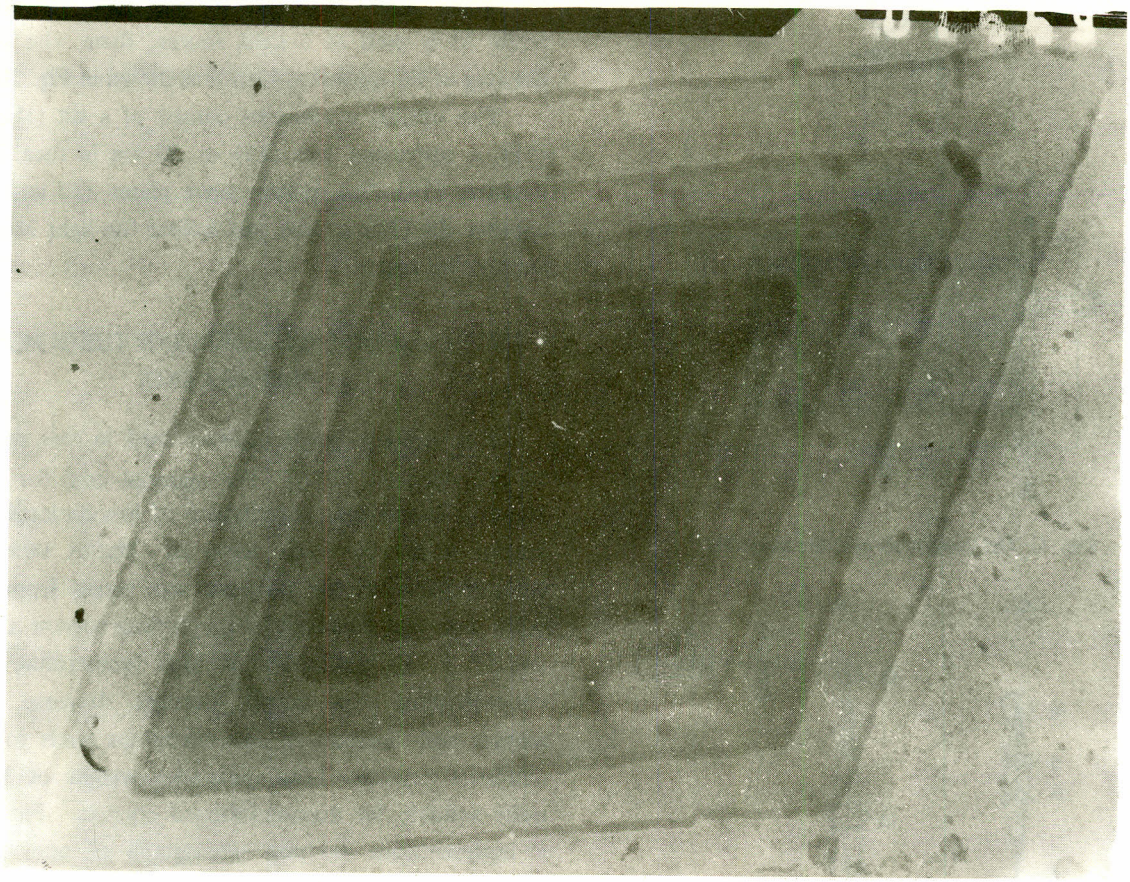

Fig. 3. Shape of the single crystals of polyethylene studied.

EXPERIMENTAL SET-UP FOR LIGHT SCATTERING AND RESULTS

Figure 4 defines those symbols which pertain to the experimental variables involved. $\vec{R}$ represents the incident beam. The axis of the concentric cylinder apparatus is parallel to $\vec{R}$. O is the location of the solution or of the dispersed systems containing the light scattering bodies. $\vec{V}$ and $\vec{G}$ are the direction of flow and of velocity gradient respectively. $\gamma = 180^{o} - \theta$, here θ is the angle of observation with respect to $\vec{R}$. ω is the angle of observation with respect to $\vec{V}$ projected into the $\vec{V} - \vec{G}$ plane.

Figure 5 represents the fractional increase in scattering due to hydrodynamic orientation at angles $\theta = \omega = 90^{o}$, by using a perpendicularly polarized laser incident light. Similar types of plots can be obtained for other ω-values which was varied from 80^{o} to 100^{o} at an interval of 3^{o} to 5^{o}. All the measurements were done at fairly constant temperature of 24 ± 1^{o}. The gap width of the annuals used in these measurements was 0.639 mm. The plot is for $\Delta I/I_R$ vs. G, where

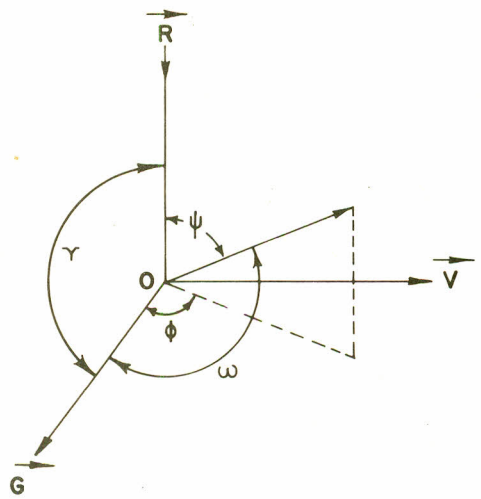

Fig. 4. Geometry of the flow arrangement considered.

$$\left[\frac{\Delta I}{I_R}\right]_{\theta=90;\omega} = \frac{(I_S)_G - (I_R)_{G=o}}{(I_R)_{G=0} - (I_W + I_{B.R.})_{G=O}}$$

$(I_S)_G$ = intensity of the light scattered at a shear G. I_R = intensity of the light scattered by the system at rest. I_W = intensity of the light scattered by water at zero shear. $I_{B.R.}$ = intensity of the light scattered due to

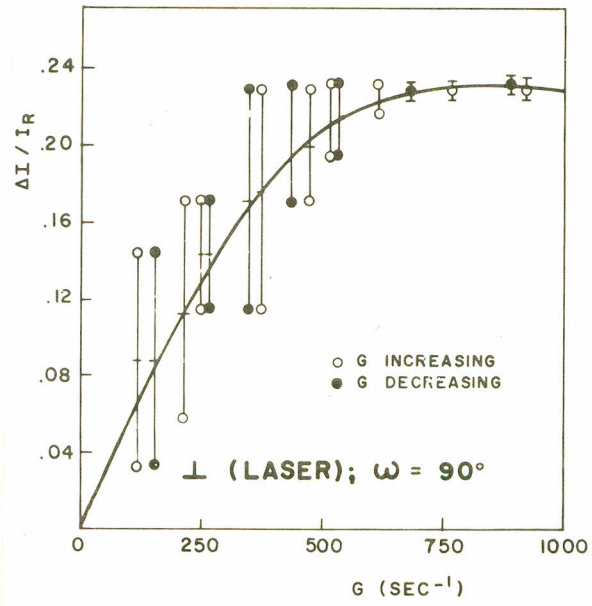

Fig. 5. Increment in intensity with shear for polyethylene crystals.

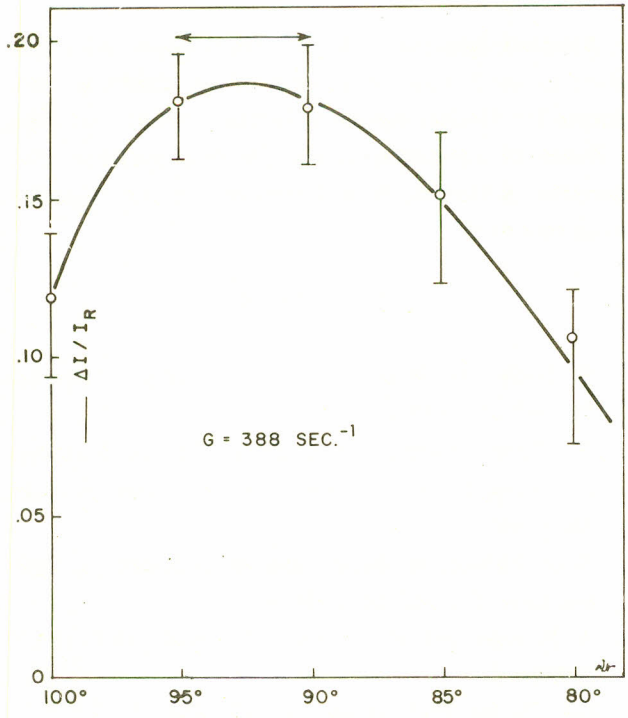

Fig. 6. 'Angular spectrum' for polyethylene crystals.

back reflection from the wall of the cylinder. Also $(I_W)_{G=o} = (I_W)_G$ because of the negligible change of the scattered light intensity due to shear. $(I_{B.R.})_{G=o}$ has been approximated to $(I_{B.R.})_G$ because of the unavailability of these values at different shear rates. The bars represents the experimental fluctuation in the data.

An angular spectrum is obtained at a fixed shear

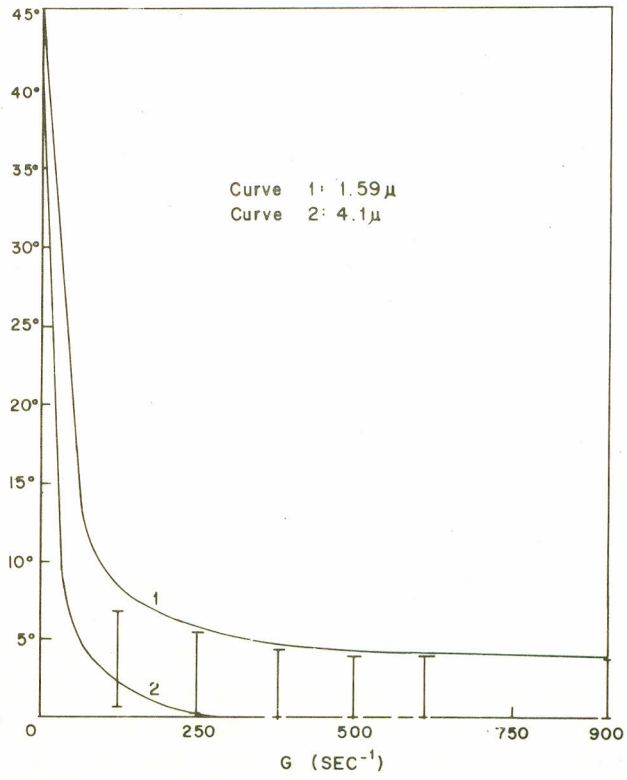

Fig. 7. 'Extinction angle' vs. gradient for polyethylene crystals.

Table 2. Maximum and minimum lengths of the different samples of polyethylene by using both Hg-arc lamp (λ = 5461 Å) and laser (λ = 6328 Å) as a light source.

Sample	L_{max} μ	L_{min} μ	Light source
I	7.51	2.83	Hg-arc
	7.39	2.91	Laser
II	5.65	2.14	Hg-arc
	5.28	2.21	Laser
III	4.74	1.95	Hg-arc
	4.43	2.10	Laser
IV	4.49	1.87	Hg-arc
	4.33	1.94	Laser
V	4.28	1.55	Hg-arc
	4.10	1.59	Laser
VI	3.97	1.51	Hg-arc
	3.91	1.54	Laser

rate from the increment values obtained at various values of ω as shown in Fig. 6. These maxima positions at various shear rates yield a χ vs. G plot, as shown in Fig. 7, where $\chi = \omega_{max} - 90^o$

Considering a prolate spheroid (the shape assumed for polyethylene crystals in this investigation), one will find that χ defines the most probable direction of its symmetry axis while ω_{max} defines the direction perpendicular to it. Consequently χ decreases from a value of 45^o as $\beta \to 0$ to 0^o as $\beta \to \infty$, ($(\beta = G/D_r)$; while ω_{max} at the same time decreases from 135^o to 90^o [11]. The bars in Fig. 7 represent the spread of the maximum, and also give the spread of the size of the system. The results of th various samples are given in Table 2.

DISCUSSION OF EXPERIMENTAL RESULTS

Figure 5 shows the variation of the flow-induced fractional increase in light scattering with the velocity gradient *G*, on observing the very thin liquid layer, contained in 0.639 mm gap. Laminar flow produces a maximal fractional increase in scattering which finally levels off. There is some fluctuation in the change in intensity at a fixed shear rate, which is considerably less than was in the case of the crystals prepared at lower temperatures and higher concentrations, and which can be attributed to two of the following reasons. (i) Either big particles pass by and cause this fluctuation (ii) or particles rotate around themsleves due to very small axial ratios and being quite bulky around its centre. This should vanish on making the solution more viscous. The result of this increase in viscosity, was the decrease in fluctuation and not complete vanishing. Possibly, by preparing the crystals of uniform size and somehow eliminating the very big crystals might bring these fluctuations to the limit of experimental uncertainty of the data. This strong effect in systems whose solid concentration was only 0.01 - 0.5% demonstrates the remarkably high sensitivity of the method to deviations in the shape of scattering objects from spherical symmetry.

Similar shaped curves were obtained for a series of other ω-values than $\omega = 90^o$ (the angles θ and φ were held constant at 90^o). However, the numerical $(\Delta I/I_R)$ values, obtained at a given *G*, varied appreciably with ω. From a series of such measurements the $(\Delta I/I_R)$ vs. ω "angular spectrum" could be obtained. This function should and did exhibit a maximum at the ω -value at which observation is perpendicular to the most probable direction of orientation of the major axis. This characteristic ω-value which was within the experimentally accessible range of angles varied necessarily with G. Also the sharpness of the maximum increased at high shear rates. This variation and sharpness of the maximum is seen in Fig. 6 where the angle $\chi = \omega_{max} - 90^o$ is used for the easy comparison with streaming birefringence results. The agreement between calculated and most probable observed χ -values is seen to be fairly good. However, the agreement varies systematically with *G*, the calculated values being too high at low *G-values* and too low at high velocity gradients. This can be easily understood as a result of finite size distribution.

The results of the sizes of the different preparations studied (Table 2) by both the light sources have a remarkable agreement to those obtained by electron microscopy (Table 1).

Acknowledgement. We are thankful to Dr. J.H.L. Watson of the Physics Department of the Edsdel B. Ford Institute for Medical Research, Detroit, U.S.A., and Frau E. Huber of Laboratorium für Elektronen-mikroskopie, Universität Karlsruhe, West Germany, for the electron microscopic work.

REFERENCES

1. W. Heller, W. Wada, and L.A. Papazian, J. Polymer Sci., **47**, 481 (1960).
2. W. Heller, Reviews Mod. Phys., **31**, 1072 (1959).
3. H.J. Doppke, and W. Heller, J. Coll. Inter. Sci., **25**, 586 (1967).
4. Noor Ahmad, W. Heller, and M. Nakagaki, J. Coll., and Inter. Sci. **31**, 585 (1969).
5. A. Peterlin, and H.A. Stuart, Z. Physik, **112** (1) 129 (1939).
6. G.I. Taylor, Phil. Trans., A 223, 289 (1923); Proc. Roy. Soc., **A102**, 541 (1923); ibid., **A157**, 546 (1936).
7. H.A. Scheraga, J.T. Edsall, and J.O. Gadd, J. Chem. Phys., **19** (9), 1101 (1951).
8. R. Gans, Ann. Physik, **86** (4), 628 (1929).
9. P.H. Geil, *Polymer Single Crystals* (Intersciences, New York, 1963).
10. D.C. Bassett, and A. Keller, Phil., Mag., **7**, 1553 (1962)
11. See equation 18 of Ref 7.